Chapter 2
Literature Review

2.1 Introduction

In order to achieve the research objectives listed in Chapter 1, an extensive literature review was conducted on material characterization of fiber reinforced polymer (FRP) beams, flexural response and failure modes of FRP and steel beams with and without openings, and different analytical methods available for characterization of flexural characteristics of FRP beams. The mechanical behavior of a FRP composite mainly depends on the fiber strength and modulus, the chemical stability, matrix strength and interface bonding between the fiber/matrix to enable stress transfer (Erden, 2010). Proper designing of composites with appropriate fiber orientation and type of fibers can produce properties equivalent to steel.

Nowadays, FRP thin-walled plated sections have found various applications in civil engineering structures such as main load carrying members of platforms, stepladder, and bridges. Generally, pultrusion technique is used to manufacture FRP beams at large scale, because it is easy and economical manufacturing process than the other techniques (Bank, 2006). In the pultrusion technique, fabrics and fibers such as chopped strand mat, continuous strand mats and rovings are pulled through a resin bath and a heated die to form the cured profile (Barbero and Raftoyiannis, 1990). Chopped strand and continuous strand mat (woven fabrics) provides strength and stiffness in longitudinal and transverse direction of the beam, as well as it provides the tearing strength to web-flange junction. In contrast, major role of rovings is to provide strength and stiffness in the longitudinal direction (Meyer, 1985). Due to the different types of fibers available, designers have many options to design beams having different properties. Hence, as per the requirement strength, the stiffness, durability, corrosion resistance, temperature resistance, etc, can be achieved. Earlier the cost of manufacturing of pultruded beams was high, but gradually research on these materials have changed the manufacturing process and design, which led to the faster and low cost of production of FRP profiles using pultrusion technique. Even though the cost of production is reduced with enhancement of the technology, the lack of standard design guidelines hinders the use of FRP beams in construction.

2.2 Fibers

Carbon and glass fibers are mostly used in FRP composites for civil engineering applications and the literature review on these fibers is explained in the following sections.

2.2.1 Carbon fibers

Carbon fibers are also called graphite fibers, but only difference between these two is that the graphite fibers have carbon content more than 99%, while carbon fibers have carbon content in the range of 80-95%. Graphite structure consists of hexagonally packed carbon atoms in layers, and several such layers are interconnected through weak van der Waals forces. Thus, such a structure generates high in-plane modulus and significantly less modulus in out-of-plane direction. In 1960, carbon fiber was discovered and it was manufactured with rayon as precursor to obtain 99% carbon content, which exhibits high strength and stiffness (Shindo, 1964 and; Tang and Bacon, 1964). Rayon is regenerated cellulose fiber produced from naturally occurring polymers. The thermal conductivity of rayon-based fibers is very low, therefore, it is useful for heat insulating materials. But the final cost of carbon fiber is very high. Later with the invention of Pan based carbon fiber, there has been little reduction in the cost, and still its cost is high in comparison with other fibers available (Tang and Bacon, 1964). Further, carbon fibers were produced from pitch precursor. Pitch fibers made from petroleum or coal tar, have high stiffness and low coefficient of thermal expansion. Carbon fiber composites made from pitch precursor are highly useful in spacecraft applications which requires thermal insulation in electronic instrumentation housings. Typical important properties of different carbon fibers obtained from different precursors are presented in Table 2.1. Nowadays, rayon type of fibers is rarely used in engineering applications (Lee, 1990).

Table 2.1 Properties of graphite fibers (Tiwari, 2005).

Property	**Pan**	**Pitch**	**Rayon**
Fiber diameter (μ)	5 to 8	10-11	6.5
Specific gravity	1.71 -1.96	2.0-2.2	1.7
Tensile modulus (GPa)	230-595	170-980	415-550
Tensile strength (MPa)	1925-6200	2275-4060	2070-2760
Elongation at failure (%)	0.40-1.20	0.25-0.70	-
Coefficient of thermal expansion (-1^{-06}/C)	0.75-0.40	1.6-0.90	-
Thermal conductivity (W/m-K)	20-80	400-1100	-

Even though initial cost of carbon fibers is high, but carbon fibers offer the highest specific modulus and strength among all reinforcing fibers (Smith, 1987). Alongwith carbon fiber laminates are chemically inert, good thermal and electrical conductors, and have low thermal expansion coefficient due to which it is ideally suited for high temperature applications (Donnet and Bansal, 1990). There is a broad range of stiffness of carbon fibers. The mechanical properties of fibers also depend on the thermal treatment of fibers as well as the tensioning of fibers during final manufacturing process. Because stiffness of carbon fibers is controlled by thermal treatment of carbon fibers. Hence, carbon fibers offer broad range of stiffness and strength as presented in Table 2.2. Surface treatment has significant effect on the interlaminar shear strength (ILSS) of carbon fibers. Because in absence of surface treatment matrix adhesion is weak, hence the bonding between fiber and matrix is weak. Therefore, it is necessary for surface treatment of fibers to improve the bonding between fiber and matrix (Bansal and Chhabra, 1981; Fitzer, 1989; Jacobasch et al., 1995; Weitzsacker and Drzal, 1996; Sherwood, 1996). Carbon fibers are mainly used as carbon fiber reinforced polymers and carbon fiber reinforced cement. Applications where cost is more important than the strength, glass fibers find potential applications.

Table 2.2 Classification of carbon fibers as per Young's modulus (Barbero, 1999).

Denomination	**Symbol**	**Young's Modulus (GPa)**
High tenacity	HT	above 3
Super high tenacity	SHT	above 4.5
Low modulus	LM	Below 200
Standard modulus	SM	200-250
Intermediate modulus	IM	250-350
High modulus	HM	350-450
Ultrahigh modulus	UHM	above 450

2.2.2 Glass fibers

The laminates made from glass fibers are ideally suited for civil engineering applications (Bakis et al., 2002), due to the low cost, high strength, and environmentally resistant. The high strength of the glass fibers is attributed to the low number and size of defects on the surface of the fiber. All types of glass fibers have approximate similar stiffness but exhibit different strength and resistance to environmental degradation. For example, S-glass has higher strength than E-glass, but E-glass is more corrosion resistant than S-glass fibers. Similarly, C-glass is highly corrosion resistant and D-glass is mainly

found in electrical applications, where high insulation is required (Barbero, 1999). Strength of glass fiber further depends on the time for immersion in chemicals, operating temperature, and application of loads. The resistance of GFRP composite to corrosion depends on the properties of fibers and matrix (Barbero and Damiani, 2003a and 2003b). ASTM D3379 (1989) specifies the procedure for determination of strength of glass fibers. Lee (1990) specifies that strength of the single fiber is not similar to strength of the fibers in composite. The reduction in strength is attributed to the residual stresses and secondary stresses produced from the matrix.

2.3 Material characterization of beams

Pultruded beams manufactured by different manufacturers have different types of fibers and resins, so it is mandatory to find the strength, stiffness and failure characteristics of pultruded beams. Stiffness and strength of pultruded beams can be determined by various self-developed methods as well as ASTM standards. The review of some of the notable publications on experimental and analytical methods for determination of the material properties of the beams is described in the following sections:

2.3.1 Experimental methods

Accurate prediction of mechanical and physical properties of FRP beams is very important for determination of flexural response and failure modes using analytical equations and numerical model. From the design prospect, designing of a structure with inaccurate properties leads to prior failure of the structure. Therefore, previous research carried out on different experimental and analytical methods is reviewed first. Like in steel, tensile and compressive characteristics of composites is determined by tensile and compression testing of coupons, respectively, however, there are different methods available to determine shear modulus and strength. All these methods are explained next.

Jones (1975) recommended the method to determine Young's modulus which is based on tensile testing of coupons as per the ASTM standard D638 (2002), and the specimens shape should be rectangular or dog bone. In order to measure longitudinal elastic modulus, fiber orientation should be along the length of the specimen and for the transverse modulus fiber orientation should be transverse to the longitudinal direction during tensile testing of specimens, while load is offered along the longitudinal direction. To determine the shear modulus, Young's modulus of specimen having fiber orientation 45^{o} to longitudinal axis has to be determined first and further shear modulus can be determined using the below equation.

$$G_{12} = \frac{1}{\frac{4}{E_x} - \frac{1}{E_1} - \frac{1}{E_2} + \frac{2\nu_{12}}{E_1}} \tag{2.1}$$

where ν_{12} is the Poisson's ratio of the material, E_x, E_1 and E_2 are the Young's moduli of specimen having fiber orientation of 0^o, 45^o and 90^o with respect to the longitudinal axis of the beam, respectively.

Fischer et al. (1981) described that Young's and shear moduli can be determined simultaneously through three-point bending test of beams and shear effect is significant in beams having low span-to-depth ratios. Authors determined the relation between deflection of beam, applied load and stiffness (E and G), after solving the deflection equations. This empirical relation was used to the measure the Young's and shear moduli of the beams. In this method, they have determined the stiffness of the full beam not the stiffness of the panels, i.e., flange and web. Hence, this method considers the warping effect and other secondary stresses produced under the three-point loading and is more accurate than the tensile and flexural testing of coupons.

Wagner et al. (1981) performed the three-point bending test of beams to examine the Young's and shear moduli and also predicted the same via empirical equations (Gere and Timoshenko, 1973 and Hard et al., 1980). Authors concluded that the errors in measurement of stiffness was due to the indentation produced by rollers on flanges. The indentation stiffness of flange increases with increasing the fiber volume fraction of flange. The measured indention stiffness from tests was compared with analytical equations based on Tsai-Halpin's equation (Ashton et al. 1969) and a good agreement of experimental and analytical results was achieved. In another study, Wagner et al., (1982) presented different equations to determine the stiffness of the beams for different types of loading configurations and beams such as cantilever and fixed-end beams.

Tolf and Clarin (1984) stated that flexural modulus obtained from three-point bending test of beams was different from tensile testing and three-point bending test of coupons due to the absence of shear deformation effect while calculating the stiffness from tensile testing and three-point bending test of coupons. Later, Corriea et al. (2011) and Correia (2012) have also confirmed that significant variation in stiffness obtained from tensile and flexural testing of coupons.

Bank (1989) investigated the Young's and shear moduli of FRP pultruded I-beams using three-point bending test. Based on Timoshenko beam theory, maximum deflection equation of the beam in terms Young's and shear moduli was determined. Author rearranged the maximum deflection equation of

the beam and obtained an equation of straight line (Eq. 2.2), which is directly related to the shear and flexural moduli of the beam. Flexural modulus is determined from the slope of the straight line, while the shear modulus is calculated from the intercept of the straight line.

$$\frac{4Aw}{Pl} = \frac{1}{12E_b}\left(\frac{l}{r}\right)^2 + \frac{1}{G_b} \tag{2.2}$$

where A is the area of web, w is the deflection of the beam, P is the applied load, l is the span length, E_b is the elastic modulus of the beam, r is the radius of gyration and G_b is the shear modulus of the beam.

Boukhili et al. (1992) studied that flexural and shear properties of the pultruded beams considering the effect of rate of loading and different span-to-depth ratios. They have reported that the effect of loading rate was more in glass fiber/polyester than in glass fiber/epoxy beams, because polyester resin is more ductile than the epoxy resin and, consequently is more loading rate sensitive. For intermediate span-to-depth ratios, the maximum load results in a tensile fracture at low loading rate and a shear fracture at high loading rate. The increase in loading rate increases the brittleness of the material, thereby increasing the sensitivity to existing defects and leading to a shear fracture rather than to a tensile fracture.

Craddock and Yen (1993) determined the mechanical properties of CFRP beams of different layups, which were fabricated by hot press system, and extra care was taken for fabrication of beams to reduce the errors. Elastic modulus was also calculated from classical lamination theory and the results obtained from theories and three-point bending testing of full section of beams was in close agreement. Authors concluded that the elimination of errors in fabrication and testing of samples achieved the good comparison of results with lamination beam theory.

Brooks and Turvey (1995) have measured the flexural rigidity of beams by uniaxial tensile testing of coupons and three-point bending test of I- and H-beams. They have shown that significant difference between the Young's modulus obtained from the tension and flexural testing. Moreover, longitudinal and transverse flexural moduli obtained from major and minor axis bending testing of beams were similar, while the shear modulus was different.

Roberts and Ubaidi (2002) have determined the flexural rigidities from 3-point and 4-point bending test and show the good agreement of results. Authors also concluded that the variation in major and minor axis shear rigidities obtained from three-point bending test were due to the different area of the

cross-section resisting the transverse shear, and different fiber content and orientation in the web and flanges. Alongwith, the Saint-Venant torsional shear modulus obtained from uniform torsion testing was significantly higher than the transverse shear modulus obtained from the major axis three-point bending test (thickness in the direction of loading), while the warping torsional modulus determined from non-uniform torsion was closer to the modulus obtained from minor axis bending (width is in the direction of loading).

Roberts and Masri (2003) also confirmed that the elastic modulus obtained from 3-point and 4-point bending tests was similar, while the shear modulus obtained from torsion testing was higher than that obtained from 3-point bending tests. But the shear modulus predicted from the deflection was higher than that determined from torsion testing. Alongwith, it was also observed that Young's modulus predicted from tensile testing of coupons was significantly different from flexural modulus obtained from three-point and four-point bending test of beams. Authors have concluded that the difference in the stiffness obtained from coupons testing and full-section testing of beams was due to the local deformation at the supports and/or under loading. The same conclusion is also observed from the study of Neto and Rovere (2007). Authors reported that the Young's modulus obtained from three-point bending test of coupons was different from those obtained from uni-axial tension and three-point bending test of full length of pultruded beams.

Minghini et al. (2012 and 2014) have proposed the different positions of loading in four-point bending test of beams for determining the flexural and shear rigidities. From the experimental investigation, they have concluded that the coefficient of variation for shear modulus predicted from proposed loading was very less as compared to modulus obtained from three- and conventional four-point bending tests. In the proposed method, flexural modulus was determined based on pure bending, while to calculate the shear modulus, span-to-depth ratio was kept low. Hence, error in prediction of stiffness was less and reliability of the results was more.

The two-rail shear (ASTM D4255, 1983), Iosipescu shear (ASTM D5379, 1993) and the V-Notched rail shear (ASTM D7078, 2005) and three-point bending (ASTM D2344, 2000) tests are ASTM standard methods for determination of shear strength of the specimens. In these methods, shear strength of the beams is determined by testing of small coupons, extruded from the beams. Earlier researchers used two-rail shear test to measure the strength and stiffness of the laminate. In this test, four pieces of rails are bolted together along the one edge of two different laminae as shown in Fig. 2.1(a) One pair of rails protrudes at the top of the laminate and the other pair at the bottom. Compression or tension is applied on the two opposite edges of the laminate, due to which shear is

induced in the laminate. In early 1960s, the Iosipescu shear test method was initially used for isotropic materials such as metals by Iosipescu (1967). Later, Iosipescu shear test fixture (see Fig. 2.1(b)) was used to measure shear strength of the composite materials (Adams and Walrath, 1985 and 1987), and in 1993 it was standardized as ASTM standard D5379 (1993). Mainly two demerits are observed in this fixture such as stress concentration at edges due to the concentrated load, which lead to the crushing of edge and additional stresses also develop in the gauge region. Another demerit is the small size of gauge section of the specimen, it is smaller than the specimen of two-rail shear test method. Later in 2005, another shear test method was developed, which contains the attractive features of the traditional methods (Iosipescu and two-rail shear tests) and is known as V-notched rail shear test method as shown in Fig. 2.1(c). In this method, specimen have V-notches, which result in a relatively uniform shear stress state within the gauge section between the notches. Two-rails are loaded on the face, which eliminate the problem of edge crushing. The three-point bending testing of short specimen as per ASTM standard D2344 (2000) is very popular nowadays. Because it is economical and easy to perform. In this test, specimen span-to-depth ratio is 6 and width-to-thickness ratio is 2. During three-point bending, specimen fails due to interlaminar shear failure, i.e., delamination (see Fig. 2.1(d)). Test set-up of short three-point bending test of composite specimen is shown in Fig. 2.1(d).

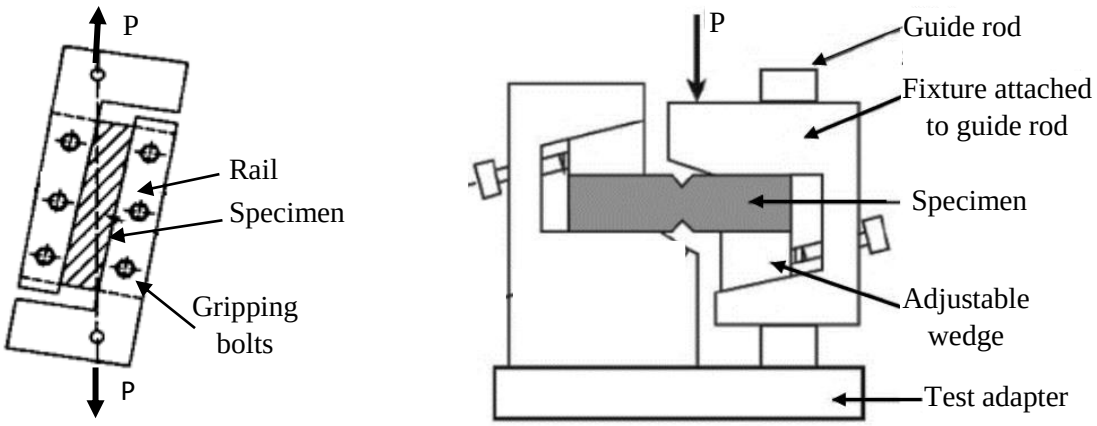

(a) Rail shear test (b) Iosipescu shear test

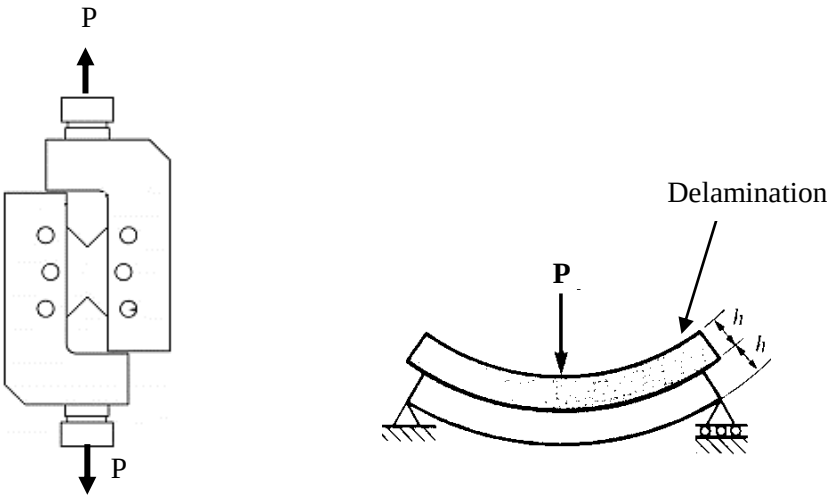

(c) V-notched rail shear test (d) Three-point bending test

Fig. 2.1. Shear test apparatus for composite specimens.

Bank (1990) have carried out an experimental study to determine the shear modulus and strength from the Iosipescu shear test method (ASTM D5379). Author determined the shear modulus by two methods. In the first method, a plot of shear stress-vs-shear strain was made. A linear regression analysis was performed from the 0% strain to the strain having a correlation coefficient of 0.995, while the shear modulus was predicted from the slope of this line. In another method, load-vs-deflection curve was plotted and the slope of the initial portion of the curve was determined and normalized with respect to the specimen's cross-sectional area. Shear modulus obtained from both methods gives the good correlation of results. The predicted shear modulus value of their beams was 2.48 ± 0.23 GPa for vinylester beams and (2.03 ± 0.19 GPa) for polyester beams.

Feraboli and Kedward (2003) have modelled the four-point bending test of short FRP specimens in ANSYS and validated with experimental results of uni-directional laminates. It is observed that failure mode (delamination) obtained from the software is similar to that obtained from experimental investigation. Further, they determined the interlaminar shear strength for multidirectional laminates such as cross-ply and quasi-isotropic laminates. They have also examined the variation of shear stresses in the skewed profile along the length, width, through the thickness, as well as the location of occurrence of delamination initiation and propagation.

2.3.2 Analytical methods

Few researchers have determined the elastic properties of pultruded beams by micromechanics approach. They have measured the stiffness of all plies of flanges and web; then combined the stiffness to obtain the full section properties. Hashin and Rosen (1964) have determined the shear

stiffness of a lamina by composite cylinder model. Luciano and Barbero (1994) have proposed a method to determine the shear stiffness and Young's modulus of a lamina based on periodic microstructure. This method is well suited to predict the shear stiffness of continuous strand mat (CSM). These two methods, i.e., composite cylinder and periodic microstructure models followed by Davalos et al. (1996) have shown that the shear stiffness calculated by these two models is higher than that obtained by the rule of mixture (Jones, 1975). Ning (1996) has used Manera method (Hashin and Rosen, 1964), which is nothing but the modified rule of mixture.

Davalos et al. (1996) have proposed a laminated beam theory to calculate the stiffness of beam from stiffness of plies. An analytical model was made, which determines the stiffnesses, stresses and strains of the plies of the laminate, including rovings, chopped and continuous strand mats, and cross- and angle-ply fabrics. In the model, coupling of the beam due to un-symmetrical layup is also considered for calculating stiffness of the beams. Further, results were verified with experimental investigation. They have shown that strains and displacement of H- and box-sections predicted from analytical models are in good agreement with experimental results.

Nagaraj and GangaRao (1997) have presented an analytical model based on the approximate classical lamination theory. They have explained the method to calculate the lamina properties, stiffness of panel and the combined stiffness of beam. Predicted stiffness from this method is closer to the experimental one. In this model, coupling produced in beams due to unsymmetrical layup is missing, but it is considered in analytical model of Davalos et al. (2006). Further, Howard (2008) also used the classical lamination theory for prediction of shear modulus of cellular beams and also used the shear modulus to predict the torsional constant 'J' from torsional rigidity.

After an extensive literature review, it is observed that little work has been done on the validation of measured stiffness from experimental tests with analytical methods. There are lot of tests to determine the Young's modulus of FRP components but its detailed comparison with analytical studies is still missing. Along with Young's modulus, shear modulus also plays a major role in the deformation of FRP I-beams. Therefore, to reproduce the behavior of FRP beams using theoretical or numerical analyses, it is important to assess the accuracy of Young's and shear moduli obtained from tests.

2.4 Flexural response of the pultruded I-beams

When symmetrical FRP I-beams are loaded in the plane of symmetry they may deflect in the symmetry plane and fails at web-flange junction and/or buckle locally or due to lateral-torsional buckling at a certain applied load. These failure modes depend on the aspect ratio of the beam (cross-

section and length), fiber orientation and properties of the beams. The behavior of FRP beams under flexural loading have been studied by several researchers over the past few decades. The flexural behavior of FRP beams is explained in the following sections:

2.4.1 Lateral-torsional buckling

Like thin-walled steel I-beams, FRP beams are susceptible to fail by local or lateral-torsional buckling. Various researchers have determined the local and lateral-torsional buckling load of beams using experimental investigation and also made the analytical and numerical models with and without consideration of shear deformation. Barbero and Raftoyiannis (1994) performed the flexural testing of pultruded beams and concluded that local buckling of compression flange was the first failure mode of the beams. Using the micromechanics approach, analytical model was made, which incorporates the effect of buckling. It is observed that critical buckling load increases with increase in the fiber orientation, i.e., 0^o to 30^o, and it decreases with further increase in the fiber orientation from 30^o to 90^o.

Mottram (1992) determined the critical buckling load using the analytical expression given in the European code (1988) and verified with the experimental results. It is noted that for the value of shear modulus of 1.2 GPa, the calculated buckling load is 14.6% higher than experimental one, while for shear modulus of 2.3 GPa, the calculated critical buckling load is 29% higher than experimental value. From the analytical model, author found that if the warping was allowed in the beams, then the predicted buckling load was approximately half than of the experimental buckling load. This is an important finding and is highly useful in designing of the structures for lateral-torsional buckling.

Barbero and Raftoyiannis (1993) stated that each part of the flanges of columns or beams can be analyzed as a plate and flange-web connection can be assumed as a rigid flange-web connection with rigid web (clamped); rigid flange-web connection with flexible web (elastic); and hinged flange-web connection. Using this approach, the predicted analytical response has excellent correlation with that of experimental.

Barbero and Raftoyiannis (1994) studied the lateral and distortional buckling of composite FRP I-beams using the equations of isotropic I-sections presented by Roberts and Jhita (1983). In the analytical model, the stability equilibrium equation of the system was established based on the minimizing the second variation of the total potential energy. Plate theory was used to consider the effect of shear and bending-twisting-coupling and to allow distortion of the cross sections.

Pandey et al. (1995) presented a theoretical formulation for determining the flexural-torsional buckling of thin-walled composite I-beams with an aim to optimize the fiber orientation. The simplified formulae based on vlasov-type linear hypothesis was derived, which accounts the beam stiffness coefficients, cross-section geometry and the material anisotropy of the section as well as the geometrical characteristics of beams. In the parametric study, different loading and boundary conditions were considered such as uniformly distributed load, transverse concentrated load, unequal end moments, tip-loaded cantilever and columns with different types of loading. They concluded that the lateral-torsional buckling load depends on the fiber orientation in web of I-beam. For concentrated load, the maximum critical buckling load was obtained at web fiber angles 0^o and 45^o for simply supported and cantilever boundary conditions of the beams, respectively. In case of end-moment, the critical buckling load was maximum at fiber orientation of 45^o for simply supported, warping restrained, lateral bending restrained, and completely fixed end beams.

Turvey (1996) conducted an experimental investigation of GFRP cantilever I-beams having span length varies from 0.5 to 1.5 m. The influence of the load position on lateral-torsional buckling behavior of the beams was also predicted using finite element software (ABAQUS). It is noted that lateral-torsional buckling load is higher when the load is applied at the bottom flange (compression flange) than the load applied at the top flange (tension flange). Authors also concluded that difference in the buckling load obtained from the experimental and numerical investigation was due to the error in measurement of in-plane shear modulus, pre-buckling deformation and geometrically nonlinear effects.

Davalos et al. (1996a) used the mechanics of laminated beam theory to determine the load-vs-deflection response and flexural strains of the FRP H and I-beams. This method is most suitable to find the ply failure of the beams, which is useful in incorporating the failure criterion in beams. In another study, Davalos et al. (1996b) and Qaio (1998) used the Rayleigh-Ritz method to determine the critical buckling load of pultruded beams. Tsai-hill failure criterion was used to determine the ply failure load. Fiber orientation and volume fraction of the fibers of pultruded I-beams was optimized for minimizing the vertical deflection, buckling and ply failure loads. The minimization of individual objective functions and obtaining a global criterion function was accomplished with available constrained optimization algorithms. Using this approach, the volume fraction of stitched fabrics, chopped strand mat and rovings was calculated as 10.85%, 4.11%, and 30.045%, respectively.

Further authors (Davalos and Qiao, 1997) used the energy principles and derived the total potential energy equations for instability of FRP wide flange sections using the nonlinear elastic theory. For the

analysis of lateral-distortional buckling, a fifth-order polynomial shape function was adopted to model the deformed shape of web panels. Two wide flanged beams having different material properties, but same cross-sections were tested under three-point loading for determining the flexural-torsional and lateral-distortional buckling responses. Beams were also modelled in the finite element software such as ANSYS. The load-vs-deflection responses obtained from analytical, numerical and experimental studies show the excellent agreement of results. Authors also examined experimentally as well as analytically the flexural-torsional and lateral-distortional buckling of simply supported FRP I-beams loaded at mid-span. There is good agreement between experimental and analytical results.

Kabir and Sherbourne (1998) proposed an analytical solution for the optimal fiber orientation in pultruded laminated channel section beams to resist the lateral buckling. Authors observed that beams having span-to-depth ratio ≤ 6 had maximum buckling load at fiber orientation of 0^o along the length of the beam. Moreover, for beams having span-to-depth ratio between 6 to 12 have maximum buckling value at fiber angle of $\pm 35^o$, while for span-to-depth ratio more than 12 the beam has maximum buckling load at 45^o fiber orientation.

Lee (2001) has developed an analytical model for open cross-section of laminated beams with symmetric and unsymmetrical laminates. He has obtained a relation between centroid and shear center with fiber angle of laminated beams. It is noted that the location of center of gravity and shear center changes with change in fiber orientation.

Sapkas and Kollar (2002) have presented a model which considers the transverse shear and shear deformation induced due to restrained warping, for determination of lateral-torsional buckling load of composite beams. Critical buckling load was also obtained from the finite element software such as ANSYS using four noded Mindlin shell elements having maximum element size of 20 mm. It is observed that when only considering the transverse shear deformation and neglecting the warping, buckling load is closer to that obtained from ANSYS. Authors concluded that lateral-torsional buckling load decreased with consideration of shear deformation in beams.

Based on a full section and coupon tests, Roberts and Masri (2003) have described the experimental determination of the flexural and torsional properties of a pultruded profile. They have also developed the closed-form solutions for the influence of shear deformation on global flexural, torsional, and lateral buckling of pultruded FRP profiles. They had shown that for wide flange I-profiles, pre-buckling displacement increased more than 20%.

Lee and Lee (2004) investigated the effect of fiber orientation on vertical deflection and the twist produced in the beam due to eccentric loading. Based on classical lamination theory, an analytical model was developed, which considers the coupling of flexural and torsional responses for arbitrary laminate stacking sequence configuration, i.e., unsymmetrical as well as symmetrical. The results obtained from analytical model were compared with those obtained using finite element software such as ABAQUS. It is observed that the deflection and angle of twist of the beam are minimum for stacking sequence of $[0]_{16}$ and maximum for $[0/45/90/45]_{2s}$ laminate. Results obtained from plane stress condition give good comparison of result with ABAQUS in comparison with plane strain condition. The worth noting conclusion from their study is that the minimum torsional displacement for the concentric and eccentric loadings is obtained at fiber angle of 50^{o} and 90^{o}, respectively.

Lee (2005) has presented a model based on shear deformable beam theory. He has analyzed the beam for flexural behavior under vertical load for arbitrary laminate stacking sequence configuration. It is observed that this analytical solution exhibits better results than that observed for classical beam theory. In his study, he has emphasized that there is a potential danger in analysis and design of FRP beams without including shear deformation. Shear deformation is predominant for low span-to-depth ratio and high elastic modulus-to-shear modulus ratio. Measurement of deflection is more accurate for low degrees of material anisotropy and becomes inappropriate as degree of the anisotropy of the beam is higher.

2.4.2 Web-flange junction failure

Tearing failure of the beam and columns is the key limitation of the pultruded products. This mode of failure is attributed to the high stress concentration and low compressive and shear strength of the layers at web-flange junction. Even though, fibers are continuous around the root of the web-flange junction, but localized wrinkling exists in the chopped strand mat. Moreover, at the center of the web-flange junction there is a triangular shaped (see Fig. 2.2) core of rovings, which is the weaker portion in the beams. Hence the failure of the web-flange junction of pultruded I-beams and columns is very common failure mode.

Fig. 2.2. Failure of web-flange junction (Borowicz and Bank, 2013).

According to Gray et al. (1984), concentrated loads produce localized effect on the beams, which create excessive stress and leads to localized failure of the beams. Crushing or buckling of the web occurs due to the high stress concentration. Hence, hard bearing pad should be used under the loading. Whitney and Browning (1985), have also confirmed that localized stresses are produced under the loading in three-point bending testing.

Bank and Yin (1999) identified that the failure of the compression flange-web junction, i.e., separation of compression flange from the web of pultruded beams is due to the local buckling of beams. It is noted that by increasing the strength of the web-flange junction with bidirectional fibers such as (0/90) fabrics at the junction increases the failure strength significantly and the mode of failure is delamination of layers of flange. This failure mode was observed as compression buckling of the flange.

Turvey and Zhang (2005) determined the failure strength (tearing strength) of the web-flange junction via pulling web of web-flange junction of T-specimen (see Fig. 2.3) which was extruded from pultruded I-beam. Authors reported that during testing, a small v-shaped crack was produced at the junction and width of the crack increased as the load increased. After the certain load, the shape of the crack changes from ‘v’ to ‘y’ and propagated towards the middle of the web. They have concluded that tearing strength increases with decrease in the length of the beam. In another study, Turvey and Zhang (2006a) determined the shear failure strength of the web-flange junction of the beams. Shear loading was applied on the web-flange junction of beams of different lengths (25, 40 and 60 mm) with or without notches on the flange. The role of the notch was to promote the shear failure of the web-flange junction, which was not easily achieved in the unnotched specimens. Authors observed that failure initiated in the roving-rich zone at the core of the web-flange junction. The shear failure strength of the un-notched beams was more than notched beams. Moreover, the shear failure strength

of unnotched specimens increases with increase in the length of the specimen, but it is independent on the length of notched in the specimen. Shear strength of the notched specimen having length 40 mm have 30% and 16% higher strength than 25 and 60 mm long specimens, respectively. Further Turvey and Zhang (2006b) investigated the rotational stiffness and strength of web-flange junction of wide flange pultruded beams via web bending tests. Stiffness and strength of the beams were determined for the beam of lengths 25 and 40 mm. Web of the beams was supported over the knife edge supports, which was used to provide the simply supported boundary conditions, while in five beams flange were kept free from supports and in seven beams, flanges were provided with semi-rigid connection, i.e., bolted connection. The transverse Young's modulus (transverse direction is along the depth of beam) obtained was 8.93±0.02 GPa, while the rotational stiffness per unit length was not consistent as transverse modulus obtained from tests. Further, Feo et al. (2013) determined the influence of the pull-out load distance from the edge of the specimens on the failure load of the web-flange junction of I-beam and a new definition for an ''influence zone'', which is equal to the depth of FRP member. The failure load of the beams increases with increase in the distance of application of load from the edge of the beam up to edge distance equals to 150 mm and for higher values it decreases. For specimen's edge distance up to 160 mm, cracks initiated in the form of a v-shaped at the center of the web-flange junction leading to a complete separation of the flange from the web. The specimen having edge distance equal to 200 mm, sudden failure was observed in the web-flange junction at the mid-span of the beam.

Fig. 2.3. Tensile testing of web-flange junction specimen (Turvey and Zhang, 2005a).

Borowicz and Bank (2011) determined the failure load of the deep beams with bearing plates. With addition of bearing plate, strength of the beam increased by 35% and the averaged shear stress at the failure increased from 17.4 MPa to 27.2 MPa. Authors used the AISC manual of steel construction (2005) to derive the equation of composite beams. The results obtained from the derived equation supports the experimental investigation. Later, Borowicz and Bank (2014) conducted an experimental investigation on the flexural study of FRP deep beams. Three-point bending tests were performed on

polyester and vinylester deep beams with span-to-depth ratios of 4. Authors examined that both types of beams experienced web buckling before web-flange junction failure. Authors pointed out that deep vinylester beams of the same geometry have higher buckling and ultimate load carrying capacity than polyester deep beams. Authors also presented an equation to determine the crippling load of FRP beams, which is modified Kollar plate buckling equation.

Correia et al. (2011) performed the three-point bending test of simply supported and cantilever FRP I-beams having span length varying from 1 m to 4 m, with and without lateral bracing in between the supports. The beams of span length 4 m and laterally restrained failed by the local buckling of the compression flange, while the unrestrained beams of same length failed by lateral-torsional buckling. The unrestrained beam of span lengths 1.0 and 1.44 m, failed due to the crushing of the web. On the other hands, all cantilevered beams, failed due to the lateral-torsional buckling. The analytical (Generalized beam theory) and numerical modelling of these beams using ABAQUS were performed in another study (Silva et al., 2010). It is noted that post-buckling responses obtained by analytical and numerical models are reasonably replicated the experimental response. But the post-buckling responses obtained from generalized beam theory is not accurately equals to the numerical response, especially in the advanced post-buckling stage.

Ascione and Mancusi (2013) considered that the web/flange junctions are rotationally deformable. Therefore, influence of rotational stiffness of the web/flange junction on the pre-buckling behavior of pultruded composite beams was studied. In the analytical model, it was assumed that torsional constraints applied only to the bottom or upper flange, therefore the web panel can be easily simulated by fixing a prescribed value of the corresponding torsional degree of freedom. The flexural behavior of the FRP H-section for eccentric vertical loading was investigated and it was observed that for low slenderness ratio of beams, the elastic limit of the web/flange rotation can be attained before buckling of the beam.

Mosallam et al. (2014) experimentally determined the axial and rotational stiffnesses and strengths of web-flange junctions of pultruded sections such as I and L-sections. Authors developed the relation between P-δ and M-θ, and idealized expressions were developed that can be used for accurate determination of stiffnesses of the beams. During rotation of compression flange of I-beam, longitudinal crack was produced on the web just below the flange of the beam. On the other hand, in L-section, localized deformation was observed in the interior region of the junction of the two legs, while on the exterior surface cracks were produced.

An insight into the web crippling behavior of pultruded GFRP I-beams, Chen and Wang (2015) did the experimental and numerical investigations on the web crippling strength of the beams under concentrated load. The influence of the bearing length and effect of different loading conditions such as end bearing with solid ground (Fig. 2.4(a)), interior bearing with solid ground (Fig. 2.4(b)), end-two-flange (Fig. 2.4(c)) and interior-two-flange (Fig. 2.4(d)) on the crippling strength of the beams was studied. It is observed that beams having end bearing with solid ground and end-two-flange loading conditions, 45^{o} crack occurred at web-flange junction. For the specimens loaded at the mid-span and supported over ground, wrinkling cracks in the upper portion of web under the bearing plate were produced and extended from the top flange to bottom flange in the shape of triangle as stress dispersed. On the other hand, wrinkling cracks were produced in beams having interior-two-flange loading conditions.

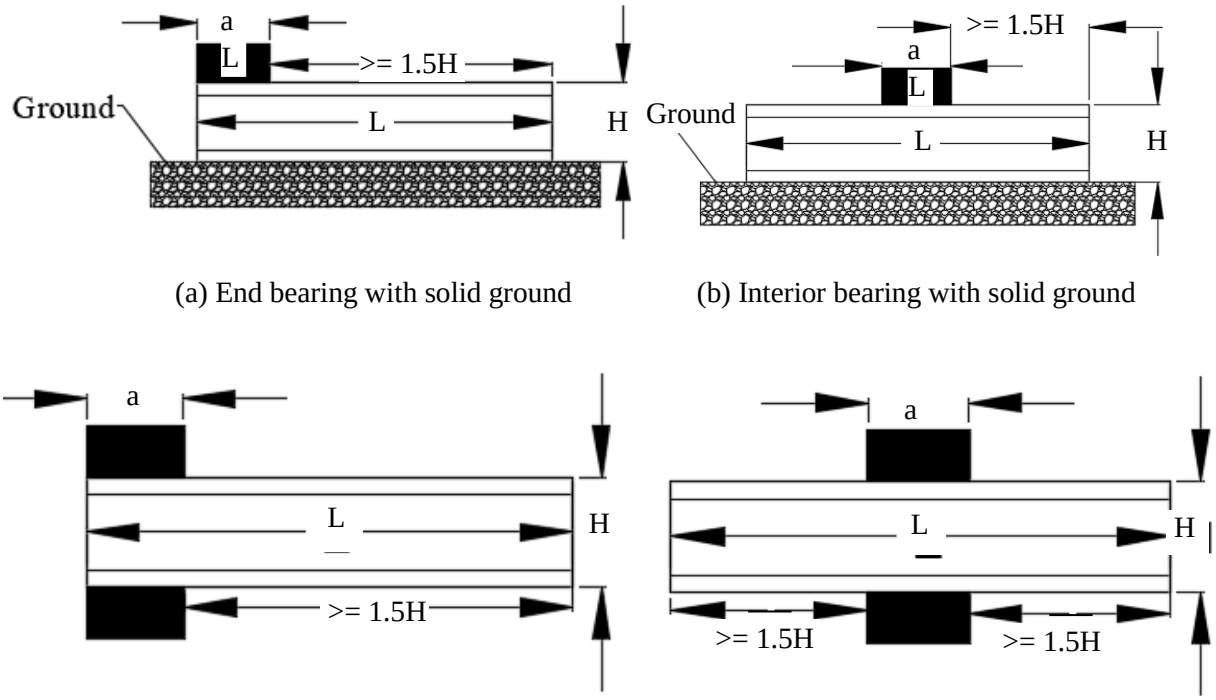

(a) End bearing with solid ground (b) Interior bearing with solid ground

(c) End-two-flange (d) Interior-two-flange

Fig. 2.4. Illustration of loading conditions.

Wu and Bai (2014) stated that slender webs experienced buckling failure, while the stocky webs experienced crushing. The ultimate load carrying capacity of the beams seated on the ground was higher than that of bearing plate.

Fernandes et al. (2015) studied the effect of bearing length on the crippling strength of the beams tested in interior-two-flanges (ITF); and end-two-flanges (ETF) loading configurations. Authors

reported that beams in which bearing length was changed from 15 mm to 100 mm, the web-crippling strength increased up to +139% and +230%, for the ITF and ETF loading configurations, respectively, while the stiffness increased up to +129% and +224%, respectively. The beams tested in ITF loading configuration, failed due to crushing of the web, except the slender beam having depth 400 mm, which failed due to local buckling of the web. Moreover, failure modes of the beams in the ITF load configuration, depends on the width of the bearing plate and depth of the beam. The beams in ITF load configuration, are very prone to local buckling of the web. Due to imperfection in the beams, failure of the web-flange junction took place before local buckling of web.

2.5 Beams with stiffening elements

Very limited study has been performed on the flexural study of FRP beams with different types of stiffening elements. In past, researchers (Bank et al., 1994 and Zureick et al., 1995) provided stiffening elements such as hollow square tube and angle section under the loading and over supports to resist the local failure. Zureick et al. (1995) reported that with addition of bearing stiffeners over supports and under loading, buckling load was 2.5 times higher than that of beam without bearing stiffener under the loading. Moreover, addition of stiffeners in between the supports and loading, the failure load was 1.05 times higher than beam having bearing stiffeners over supports and under loading.

Bank et al. (1994) studied the flexural behavior of FRP pultruded I-beams under three-point bending. To predict the local behavior of the beams, they were stiffened under loading and over supports to prevent warping and crippling. Study was performed on vinylester and polyester beams with same size and layup. It is noted that the value of the buckling stress obtained from the polyester beams is very close to that of the vinylester beams. But the strain at the event of buckling in the polyester beams is higher than that of the vinylester beams, which indicate that vinylester beams offers higher stiffness. It is observed that beams without stiffeners and bearing plate at supports failed due to the crushing of the web, while the beams having tubular bearing stiffeners failed due to the transverse buckling of the web near to the supports. In another vinylester beam, tearing failure of the compression flange-web junction was observed, which occurred due to the longitudinal crack propagated along the length of the beam at the web-flange junction. In contrast with vinylester beams, failure mode of the polyester beams was local buckling of compression flange.

The AISC Manual of Steel Construction (2005) addresses the use and design of web stiffeners to prevent web crippling. It states that a transverse stiffener, or pair of transverse stiffeners, or a doubler plate at least one-half the depth of the web shall be provided. Stiffeners are designed to resist the

compressive forces applied vertically on the stiffeners where they act like a compression member. As per the code (AISC, 2005) the effective length of the stiffener should be 0.75h (h is the height of the beam), width of the stiffeners should be $25t_w$ and $12t_w$ for the interior and end stiffener of the beam, respectively, where t_w is the thickness of web.

Borowicz and Bank (2013) investigated the flexural behavior of I-section with bearing plate under three-point bending. They have determined that beams with bearing plate have about 35% higher load carrying capacity than beams without bearing plates. However, the beams failed by failure of web-flange junction under bearing plate. In order to reduce the local failure, authors further conducted series of three-point bending tests on FRP beams with different stiffening elements such as FRP plates (over web under loading), bearing stiffeners and cover angles. Authors (Borowicz and Bank, 2013) have concluded that with addition of web plates, bearing, and cover angles, ultimate load carrying capacity increased by 31%, 53%, and 59%, respectively. It is noted that the beams with bearing plate and web plate failed by wedge-shear failure under the loading, while beams with bearing stiffeners failed at support by failure of junction.

2.6 Castellated beams

A review of the literature on castellated beams reveals that a lot research has been carried out on the steel castellated beams, but no study has been found on the FRP castellated beams. Therefore, extensive literature review is done on steel castellated beams, which is helpful for designing and fabrication of FRP castellated beams. Use of castellated beams with hexagonal or square or circular shaped openings are very common in recent years because of high depth with the same material (Boyer, 1964). Toprac and Cooke (1959) reported that under pure bending castellated beam behave like a compact section, tee sections above and below the openings yield in tension and compression until it become fully plastic. According to Amayreh and Saka (2005) different modes of failure exists in the castellated beams under flexural are as follow:

- Flexure mechanism formation
- Overall beam lateral-torsional buckling
- Web post-compression buckling
- Web post-shear bucking
- Tee compression buckling
- Vierendeel mechanism formation
- Welded joint rupture in the web

In these failure modes, first and second failure modes are similar to the failure modes of solid web I-beams (Nethercot and Kerdal, 1982). Hence, failure strength of the castellated beams can be easily predicted by equations of solid I-beams. Knowles (1991) reported that failure load predicted by assuming web-post as a column in compression using Blogett's force distribution model and an effective length factor, gives good comparison of results with the experimental results. In this approach, the web post was treated as a column having width equal to the narrowest width of the web, length was taken equal to the clear height of the castellation, and thickness equal to the web thickness. Therefore, failure strength of the castellated beams having buckling failure modes third, fourth and fifth is similar to the solid I-beams. On the other hand, modes of failure sixth to seventh are specially related to the castellated beams (Gandomi et al., 2011).

Vierendeel type of failure occurs due to the combined action of shear and moment in the castellated beam. Due to loading on castellated beam, shear induces in the both T-sections. Therefore, a moment produces in the beams which is called as the Vierendeel moment. Due to consequences of this moment, plastic hinges form at the corner of the openings and the beams deform in parallelogram shape as shown in Fig. 2.5. (Toprac and Cooke, 1959). Rupture of welded joint is due to horizontal shear stresses exceed the yield strength of the welded joint.

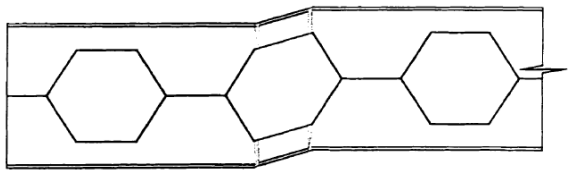

Fig. 2.5. Formation of plastic hinges at the corner of the opening.

Hosain and Spiers (1971) reported that rupture of weld depends on the length of the welded joint. The reduction in horizontal length, results in decrease in the secondary moments, which is attributed to the rupture of the welded throat of the T-sections. Later, Hosain and Spiers (1973) concluded that the failure of locally and laterally braced castellated I-sections will probably initiate either by Vierendeel mechanism or rupture of welding joint in the web due to excessive shear stress. Moreover, reducing throat length of weld, increases the chances of failure of weld and decreases the chances of formation of Vierendeel mechanism.

Zaarour and Redwood (1996) conducted three-point bending test on castellated beams with and without stiffening of weld region with plates. Rotation of flanges was observed in beams having plates over the welded portion, while the other beams without plates failed due to the web-post buckling.

Authors also stated that susceptibility to web-post buckling was due to low value of the ratio of critical buckling load/yielding load. It was observed that for beam without web plate on web, rotation of the web was associated with the rotation of the flange, while for the beams with web plate, rotation of the flanges was observed, due to local buckling.

Redwood and Demirdijan (1998) investigated the flexural behaviour of the castellated beams having four, six and eight openings. It is noted that the beams having four and six openings failed by buckling of the web, while the beams having eight openings failed due to the lateral-torsional buckling. From the finite element analysis, authors have observed that critical buckling load decreases with increase in the number of openings in the beams. Elastic buckling coefficients due to shear force at the web were also determined. Coefficients were used for modeling of the beam's end region incorporating two holes, using assumptions concerning the restraining effect of the flanges. These coefficients are applicable to ends of a simply supported beam which carries a uniformly distributed load.

Using numerical investigation, Sweedan (2011) determined the moment-gradient coefficient (C_b) of the cellular beam for concentrated and uniformly distributed loading. Alongwith, a relation between moment gradient coefficient and the warping rigidity was also predicted. It is noted that the cellular beams subjected to concentrated load at mid-span have higher strength than that of beams having uniformly distributed loads. Authors pointed out that reduction of C_b was high in short beams and excessive shear stresses were developed leading to local web distortions that occur simultaneously with lateral buckling.

Lawson et al. (2006) derived the web-post buckling equation of asymmetric beams having elongated and circular openings. From the finite element analyses, author observed that long openings cause pull-out forces in the shear connectors due to the development of local composite action. Therefore, equation of Vierendeel bending resistance was modified by multiplication with a reduction factor, which depends on the length of the opening. Authors also recommended that length-to-depth ratio of unstiffened elongated openings should not exceed 2.5.

Wang et al. (2014) performed the numerical investigation on castellated beams with fillet at the corners of hexagonal openings as shown in Fig. 2.6. Authors concluded that incorporating the fillet radius along the web opening decreases the stress concentration at the corners which ultimately enhances the strength of the castellated beams. The global bending moment capacity of the perforated member increases as the expansion ratio (height/length of opening) increases. Vertical shear capacity

of the perforated beam decreases with increasing the size of opening, because of the Vierendeel bending moment.

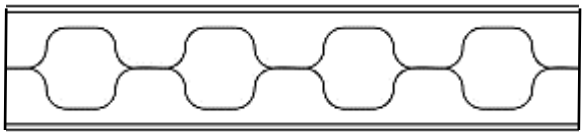

Fig. 2.6. Beam with fillet corner web opening.

2.7 Gaps in present research

The limitations and research issues identified from the current literature review are as follow:

1. There is no study performed by any author on the comparison of elastic and shear moduli of FRP beams obtained using 4-point bending test and analytical theories such as approximate classical lamination and mechanics of laminated beams theories

2. Most of the studies carried out on characterization of buckling response of FRP beams using different analytical methods. The major focus of the researchers was to develop analytical models for prediction of critical buckling load of beams and columns like in steel beams. Few studies reported the validation of numerical and analytical models with experimental tests. Verification of their models for different length-to-depth (L/d) ratios is also missing in the literature.

3. FRP beams are very prone to fail by rupture of the layers of web-flange junction. Very limited studies are available which discusses the prediction of strength of web-flange junction and reason of failure of the web-flange junction of pultruded beams.

4. Few studies have reported the use of stiffening elements to resist the failure of web-flange junction of I-beams. But the detailed investigation of different sizes of stiffening elements on the flexural strength of beams having different flange width-to-thickness (b/t) ratios, web height-to-thickness (h_w/t) ratios and L/d ratios is missing.

5. Most importantly, the effect of various stiffening elements such as carbon fiber layers, bearing plate, carbon fiber angle, web plate and cover plate on the overall flexural response, strength and failure modes is missing.

6. Hardly any researcher has ever put focus to develop a FRP castellated beams.